

# POLARIZATION OBSERVABLES IN $(\vec{e}, e'\vec{N}N)$ and $(\vec{\gamma}, \vec{N}N)$ REACTIONS<sup>†</sup>

C. Giusti and F. D. Pacati

*Dipartimento di Fisica Nucleare e Teorica, Università di Pavia,  
and Istituto Nazionale di Fisica Nucleare, Sezione di Pavia, Pavia, Italy*

Nucleon recoil polarization in electromagnetic reactions with two-nucleon emission is discussed for both  $(\vec{e}, e'\vec{N}N)$  and  $(\vec{\gamma}, \vec{N}N)$ . Numerical results are given for exclusive two-nucleon knockout reactions from  $^{16}\text{O}$  in a theoretical model where final-state interactions, one-body and two-body currents, and the effect of correlations in the initial pair wave function are included.

## I. INTRODUCTION

Electromagnetically induced two-nucleon knockout has long been devised as the most direct tool for exploring the properties of nucleon pairs within nuclei, their interaction at short distance and therefore short-range correlations (SRC) [1]. In order to extract this information, a reliable theoretical model is needed, able to keep reasonably under control the reactions processes and the various ingredients, as well as a combined experimental study of different reactions in different situations, where the various contributions play a different role and can thus be disentangled and separately investigated.

Two nucleons can be naturally ejected by two-body currents, which effectively take into account the influence of subnuclear degrees of freedom like mesons and isobars. Direct insight into SRC can be obtained from the process where the real or virtual photon hits, through a one-body current, either nucleon of a correlated pair and both nucleons are then ejected from the nucleus. A reliable and consistent treatment of these two competing processes, both produced by the exchange of mesons between nucleons, is needed. Their role and relevance, however, can be different in different reactions and kinematics. It is thus possible to envisage situations where either process is dominant and can be separately investigated.

Interesting and complementary information is available from electron and photon-induced reactions. The electron probe is however preferable for the study of SRC. In fact, two-body currents predominantly contribute to the transverse components of the nuclear response. Only these components are present in photon-induced reactions that appear thus generally dominated by two-body currents. Also the longitudinal component, dominated by correlations, is present in electron-induced reactions. The possibility of independently varying the energy and momentum transfer of the exchanged virtual photon allows one to select kinematics where the longitudinal response and thus SRC are dominant.

A combined study of  $pp$  and  $np$  knockout is needed for a complete information. Correlations are different in  $pp$  and  $np$  pairs. They are stronger in  $np$  pairs and thus in  $np$  knockout due to the tensor force, that is predominantly present in the wave function of a  $np$  pair. But also two-body currents are much more important in  $np$  knockout, while they are strongly suppressed in  $pp$  knockout, where the charge-exchange terms of the two-body current do not contribute. Therefore, the  $(e, e'pp)$  reaction was devised as the preferential process for studying SRC in nuclei. It is however clear that, since different effects can be emphasized in suitable conditions for different reactions, a combined study of  $pp$  and  $np$  knockout induced by real and virtual photons is needed to unravel the different contributions and obtain a clear and complete information on  $NN$  correlations.

Exclusive reactions, for transitions to specific discrete eigenstates of the residual nucleus, are of particular interest for this study. One of the main results of the theoretical investigation is the selectivity of exclusive reactions involving different final states that can be differently affected by one-body and two-body currents [2,3]. Thus, the experimental resolution of specific final states may act as a filter to disentangle the two reaction processes.  $^{16}\text{O}$  is a suitable target for this study, due to the presence of discrete low-lying states in the experimental spectrum of  $^{14}\text{C}$  and  $^{14}\text{N}$  well separated in energy. From this point of view,  $^{16}\text{O}$  is better than a light nucleus, which lacks specific final states.

First measurements of the exclusive  $^{16}\text{O}(e, e'pp)^{14}\text{C}$  reaction performed at NIKHEF [4–6] and MAMI [7,8] have basically confirmed the predictions of the theoretical model and have given clear evidence for SRC for the transition to the ground state of  $^{14}\text{C}$ . This result gives rise to the hope that a similar separation between two-body currents and correlations is possible also in the  $(e, e'np)$  reaction. This would be of particular interest for the study of tensor correlations. No data are available at present, but a proposal for the experimental study of the exclusive  $^{16}\text{O}(e, e'np)^{14}\text{N}$  reaction was approved in Mainz and is in preparation [9].

---

<sup>†</sup>submitted to the 5th Workshop on "e.-m. induced two-hadron emission", Lund, June 13-16, 2001.

First pioneering ( $\gamma, NN$ ) experiments were performed in Bonn [10] and Tokyo [11] with poor statistical accuracy and energy resolution. Further experiments carried out at MAMI achieved much better results [12]. These experiments, with a resolution of about 6-9 MeV, were able to resolve the major shells from which the two nucleons are emitted. The first high-resolution  $^{16}\text{O}(\gamma, np)^{14}\text{N}$  experiment able to separate final states was performed at MAXlab in Lund [13], in a small energy range and with low statistics. A high-resolution experiment for the  $^{16}\text{O}(\gamma, np)^{14}\text{N}$  and  $^{16}\text{O}(\gamma, pp)^{14}\text{C}$  reactions in the photon-energy range between 90 and 270 MeV, aiming not only at separating final states but also at determining the momentum distributions of each state, was approved in Mainz and is in preparation [14]. Results for a first test and feasibility study are presented in [15].

Good opportunities to increase the richness of information available from two-nucleon knockout are offered by polarization measurements. Reactions with polarized particles give access to a larger number of observables, hidden in the unpolarized case and whose determination can impose more severe constraints on theoretical models. Some of these observables are expected to be sensitive to the small components of the transition amplitudes, which are generally masked by the dominant ones in the unpolarized cross section. These small components often contain interesting information on subtle effects and may thus represent a stringent test of theoretical models. This is the place where polarization observables enter, because in general they contain interference terms of the various matrix elements in different ways. Thus, a small amplitude may be considerably amplified by the interference with a dominant one.

The asymmetry of the cross section for linearly polarized photons in ( $\gamma, pp$ ) and ( $\gamma, pn$ ) was studied in [16,18]. Numerical results for exclusive  $pp$  and  $pn$  knockout from  $^{16}\text{O}$  can be found in [17]. First measurements with polarized photon beams have been performed at LEGS on  $^3\text{He}$  [19] and  $^{16}\text{O}$  [20] and at MAMI on  $^{12}\text{C}$  [21]. In these experiments, however, the energy resolution was not enough to separate specific final states of the residual nucleus.

The case of the nucleon recoil polarization in ( $\vec{\epsilon}, e' \vec{N}N$ ) and ( $\vec{\gamma}, \vec{N}N$ ) reactions where also the incident electron or the incident photon is polarized is considered here. The formalism and the polarization observables for ( $\vec{\epsilon}, e' \vec{N}N$ ) and ( $\vec{\gamma}, \vec{N}N$ ) are discussed in sects. 2 and 3, respectively. Some numerical examples for exclusive knockout reactions on  $^{16}\text{O}$  are presented in sect. 4. Other examples and a more detailed discussion of the formalism are given in [22,23]. Some numerical results obtained with a different theoretical model can be found also in [18,24].

## II. FORMALISM FOR THE ( $\vec{\epsilon}, e' \vec{N}N$ ) REACTION

The triple coincidence cross section for the electron induced reaction where two nucleons, with momenta  $\mathbf{p}'_1$  and  $\mathbf{p}'_2$  and energies  $E'_1$  and  $E'_2$ , are emitted is obtained from the contraction between the lepton tensor and the hadron tensor as a linear combination of 9 structure functions [1,25]

$$\frac{d^5\sigma}{dE'_0 d\Omega'_0 d\Omega'_1 d\Omega'_2 dE'_1} = K \left\{ \epsilon_L f_{00} + f_{11} + \sqrt{\epsilon_L(1+\epsilon)}(f_{01} \cos \alpha + \bar{f}_{01} \sin \alpha) - \epsilon(f_{1-1} \cos 2\alpha + \bar{f}_{1-1} \sin 2\alpha) + h \left[ \sqrt{\epsilon_L(1-\epsilon)}(f'_{01} \sin \alpha + \bar{f}'_{01} \cos \alpha) + \sqrt{1-\epsilon^2} f'_{11} \right] \right\}, \quad (1)$$

where  $E'_0$  is the energy of the outgoing electron and  $K$  is a kinematic factor. The combination coefficients are obtained from the components of the lepton tensor and depend only on electron kinematics, with

$$\epsilon = \left( 1 + 2 \frac{|\mathbf{q}|^2}{Q^2} \tan^2 \frac{\theta}{2} \right)^{-1}, \quad \epsilon_L = \frac{Q^2}{|\mathbf{q}|^2} \epsilon, \quad (2)$$

where  $\theta$  is the electron scattering angle,  $Q^2 = |\mathbf{q}|^2 - \omega^2$ , and  $\omega$  and  $\mathbf{q}$  are the energy and momentum transfer, respectively.

The structure functions  $f$  result from suitable combinations of the components of the hadron tensor [1,25] and depend on the kinematical variables  $\omega$ ,  $q$ ,  $p'_1$ ,  $p'_2$ , on the angles  $\gamma_1$ , between  $\mathbf{p}'_1$  and  $\mathbf{q}$ ,  $\gamma_2$ , between  $\mathbf{p}'_2$  and  $\mathbf{q}$ , and  $\gamma_{12}$ , between  $\mathbf{p}'_1$  and  $\mathbf{p}'_2$ . The three structure functions  $f'$  are obtained when also the incident electron is polarized with helicity  $h$ .

The number of structure functions is reduced in particular kinematics. When the angle  $\alpha$ , between the ( $\mathbf{p}'_1, \mathbf{q}$ ) plane and the electron scattering plane, is equal to 0 or  $\pi$ , the structure functions which are multiplied by  $\sin \alpha$  or  $\sin 2\alpha$  in Eq. (1) do not contribute to the cross section. When  $\mathbf{p}'_1$ ,  $\mathbf{p}'_2$ , and  $\mathbf{q}$  lie all in the same plane, we recover the case of the ( $\vec{\epsilon}, e'N$ ) reaction and only 5 structure functions survive:  $f_{00}$ ,  $f_{11}$ ,  $f_{01}$ ,  $f_{1-1}$ ,  $f'_{01}$ . In a coplanar kinematics, where both conditions are fulfilled, only the 4 structure functions  $f_{00}$ ,  $f_{11}$ ,  $f_{01}$ ,  $f_{1-1}$  survive. In the interesting case of the super-parallel kinematics, where the two outgoing nucleons are ejected parallel and antiparallel to the momentum

transfer, only the two structure functions,  $f_{00}$  and  $f_{11}$ , survive [25], as in the parallel kinematics of  $(e, e'N)$  and in the inclusive  $(e, e')$  reaction, and in principle can be separated by a Rosenbluth plot.

If one of the two outgoing nucleons has a given polarization, the components of the hadron tensor can be written in terms of the spin density matrix, that for a nucleon can be expanded in terms of the Pauli matrices  $\boldsymbol{\sigma}$  as

$$\boldsymbol{\rho} = \frac{1}{2} \left( 1 + \mathbf{P} \cdot \boldsymbol{\sigma} \right), \quad (3)$$

where  $\mathbf{P}$  is the outgoing nucleon polarization. Thus, the components of the hadron tensor and therefore also the structure functions can be written as the sum of two parts, one independent and one dependent on  $\mathbf{P}$ . As a consequence of the spin- $\frac{1}{2}$  nature of the nucleon, the dependence on the spin is at most linear, and the nine structure functions are written as

$$f_{\lambda\lambda'} = h_{\lambda\lambda'}^u + \hat{\mathbf{s}} \cdot \mathbf{h}_{\lambda\lambda'}, \quad (4)$$

where  $\hat{\mathbf{s}}$  is the unit vector in the spin space. When the outgoing nucleon polarization is not detected and the cross section is summed over the spin quantum numbers of the outgoing nucleon, the spin independent structure functions  $h_{\lambda\lambda'}^u$  go over to the 9 structure functions  $f_{\lambda\lambda'}$  of the unpolarized case [1,22]. New structure functions are produced in the polarized case by the components of  $\mathbf{h}_{\lambda\lambda'}$ .

The quantity  $\mathbf{h}_{\lambda\lambda'}$  is usually projected onto the basis of unit vectors given by  $\hat{\mathbf{L}}$  (parallel to the momentum  $\mathbf{p}'$  of the outgoing particle),  $\hat{\mathbf{N}} = \mathbf{q} \times \mathbf{p}'$ , and  $\hat{\mathbf{S}} = \hat{\mathbf{N}} \times \hat{\mathbf{L}}$ , which define the cm helicity frame of the particle. Thus, in the most general situation there are 9 unpolarized  $h_{\lambda\lambda'}^u$  and 9 polarized  $h_{\lambda\lambda'}^i$  structure functions for each direction  $i = N, L, S$ , i.e. 36 structure functions.

The coincidence cross section of the  $(\vec{e}, e'\vec{N}N)$  reaction can be written as

$$\frac{d^5\sigma}{dE'_0 d\Omega'_0 d\Omega'_1 d\Omega'_2 dE'_1} = \sigma_0 \frac{1}{2} \left[ 1 + \mathbf{P} \cdot \hat{\mathbf{s}} + h(A + \mathbf{P}' \cdot \hat{\mathbf{s}}) \right], \quad (5)$$

where  $\sigma_0$  is the unpolarized differential cross section,  $\mathbf{P}$  the outgoing nucleon polarization,  $A$  the electron analyzing power and  $\mathbf{P}'$  the polarization transfer coefficient.

The components of  $\mathbf{P}$  and  $\mathbf{P}'$  are given by suitable combinations of the polarized structure functions, involving also the matrix elements of the lepton tensor, and divided by  $\sigma_0$ . The explicit expressions can be found in [22].

In an unrestricted kinematics all the 36 structure functions and all the components  $P^N, P^L, P^S$  and  $P'^N, P'^L, P'^S$  are allowed. This number is reduced in particular situations. The condition  $\alpha = 0$  or  $\pi$  reduces to 24 the number of structure functions. When the vectors  $\mathbf{q}, \mathbf{p}'_1, \mathbf{p}'_2$  lie in the same plane, only 18 structure functions survive, as in  $(\vec{e}, e'\vec{N})$ , and only 12 in coplanar kinematics. In this case only the components  $P^N, P'^L$  and  $P'^S$  survive, as in the coplanar kinematics of  $(\vec{e}, e'\vec{N})$ . In the super-parallel kinematics, only 5 structure functions survive, the 2 unpolarized  $h_{00}^u$  and  $h_{11}^u$  and the three  $h_{01}^N, h_{01}^S, h_{11}^L$ , and thus  $P^N, P'^L$ , and  $P'^S$  are each directly proportional to only one structure function [22].

When final-state interactions (FSI) are neglected and the plane-wave (PW) approximation is used for the outgoing nucleons wave functions,  $P^N = P^L = P^S = 0$ , while  $\mathbf{P}'$  does not vanish [22].

### III. FORMALISM FOR THE $(\vec{\gamma}, \vec{N}N)$ REACTION

For the reactions induced by a real photon, only the transverse components of the nuclear current contribute and a reduced number of structure functions is obtained. The cross section of the  $(\vec{\gamma}, NN)$  reaction is written in terms of 4 structure functions [23]

$$\frac{d^3\sigma}{d\Omega_1 d\Omega_2 dE'_2} = K_\gamma [f_{11} + \Pi_c f'_{11} - \Pi_t (f_{1-1} \cos 2\phi_\gamma - \bar{f}_{1-1} \sin 2\phi_\gamma)], \quad (6)$$

where  $K_\gamma$  is a kinematic factor,  $\Pi_c$  and  $\Pi_t$  are the degrees of circular and linear polarization of the photon and  $\phi_\gamma$  is the angle of the photon polarization vector relative to the scattering plane, i.e. the  $(\mathbf{q}, \mathbf{p}'_1)$  plane.

When the photon is not polarized, only  $f_{11}$  contributes to the cross section  $\sigma_0$ . Three more structure functions are obtained when the incident photon is circularly ( $f'_{11}$ ) and linearly ( $f_{1-1}, \bar{f}_{1-1}$ ) polarized. They can be experimentally separated measuring the circular asymmetry

$$A_c = \frac{\sigma(+)-\sigma(-)}{\sigma(+)+\sigma(-)} = \frac{f'_{11}}{f_{11}}, \quad (7)$$

where  $\sigma(+)$  and  $\sigma(-)$  are the cross sections for a circularly polarized photon and  $\Pi_t = 0$ , and the two independent linear asymmetries,

$$\Sigma_{\frac{\pi}{2}} = \frac{\sigma(0) - \sigma(\frac{\pi}{2})}{\sigma(0) + \sigma(\frac{\pi}{2})} = -\frac{f_{1-1}}{f_{11}}, \quad \Sigma_{\frac{\pi}{4}} = \frac{\sigma(\frac{\pi}{4}) - \sigma(-\frac{\pi}{4})}{\sigma(\frac{\pi}{4}) + \sigma(-\frac{\pi}{4})} = \frac{\bar{f}_{1-1}}{f_{11}}, \quad (8)$$

where  $\sigma(0)$ ,  $\sigma(\frac{\pi}{2})$  and  $\sigma(\frac{\pi}{4})$  are the cross sections for a linearly polarized photon in the directions  $\phi_\gamma = 0, \frac{\pi}{2}$ , and  $\frac{\pi}{4}$ , respectively, and  $\Pi_c = 0$ .

When the polarization of one of the two outgoing nucleons is detected, the 4 structure functions in Eq. (6) are written, like in Eq. (4), in terms of 4 spin independent,  $h_{\lambda\lambda'}^u$ , and 12 spin dependent functions  $h_{\lambda\lambda'}^i$ , 4 for each component  $i = N, L, S$ . Thus, 16 structure functions are obtained in the most general situation for the  $(\vec{\gamma}, \vec{N}N)$  reaction.

The 12 structure functions  $h_{\lambda\lambda'}^i$  are directly connected with 12 polarization observables, 4 for each direction  $N, L$ , and  $S$ . For an unpolarized photon, we have the components of the polarization

$$P^i = \frac{\sigma(+1) - \sigma(-1)}{\sigma(+1) + \sigma(-1)} = \frac{h_{11}^i}{h_{11}^u}, \quad (9)$$

where  $\sigma(+1)$  ( $\sigma(-1)$ ) are the cross sections with a nucleon polarized parallel (antiparallel) to the direction  $\hat{s}^i$ .

If the photon is circularly polarized and  $\Pi_t = 0$ , we have the components of the polarization transfer coefficient

$$P_c^i = \frac{\sigma(+, +1) - \sigma(+, -1) - \sigma(-, +1) + \sigma(-, -1)}{\sigma(+, +1) + \sigma(+, -1) + \sigma(-, +1) + \sigma(-, -1)} = \frac{h_{11}^i}{h_{11}^u}, \quad (10)$$

where the first argument in  $\sigma$  refers to the photon polarization and the second one to the nucleon polarization in the direction  $\hat{s}^i$ .

For a linearly polarized photon and  $\Pi_c = 0$ , we have the components of the two polarization asymmetries

$$\Sigma_{\frac{\pi}{2}}^i = \frac{\sigma(0, +1) - \sigma(0, -1) - \sigma(\frac{\pi}{2}, +1) + \sigma(\frac{\pi}{2}, -1)}{\sigma(0, +1) + \sigma(0, -1) + \sigma(\frac{\pi}{2}, +1) + \sigma(\frac{\pi}{2}, -1)} = -\frac{h_{1-1}^i}{h_{11}^u} \quad (11)$$

and

$$\Sigma_{\frac{\pi}{4}}^i = \frac{\sigma(\frac{\pi}{4}, +1) - \sigma(\frac{\pi}{4}, -1) - \sigma(-\frac{\pi}{4}, +1) + \sigma(-\frac{\pi}{4}, -1)}{\sigma(\frac{\pi}{4}, +1) + \sigma(\frac{\pi}{4}, -1) + \sigma(-\frac{\pi}{4}, +1) + \sigma(-\frac{\pi}{4}, -1)} = \frac{\bar{h}_{1-1}^i}{h_{11}^u}, \quad (12)$$

where the first argument in  $\sigma$  refers to the value of the angle  $\phi_\gamma$ .

In a coplanar kinematics only 8 structure functions survive:  $h_{11}^N, h_{11}^L, h_{1-1}^N, h_{1-1}^L, h_{11}^{L,S}$ , and  $\bar{h}_{1-1}^{L,S}$ , and thus only the quantities  $\sigma_0, P^N, \Sigma_{\frac{\pi}{2}}^N, \Sigma_{\frac{\pi}{2}}^L, P_c^{L,S}$ , and  $\Sigma_{\frac{\pi}{4}}^{L,S}$  can be measured. In the PW approximation only  $h_{11}^u, h_{1-1}^u, \bar{h}_{1-1}^u$ , and  $h_{11}^{N,L,S}$  survive, and therefore  $\sigma_0, \Sigma_{\frac{\pi}{2}}^N, \Sigma_{\frac{\pi}{4}}^L$ , and  $P_c^{N,L,S}$ , while  $A_c = P^{N,L,S} = \Sigma_{\frac{\pi}{2}}^{N,L,S} = \Sigma_{\frac{\pi}{4}}^{N,L,S} = 0$ .

All these results can be derived from the general properties of the components of the hadron tensor [22,23].

## IV. RESULTS

Calculations have been performed within the theoretical framework of Refs. [2,3] for exclusive  $pp$  and  $np$  knockout. In the transition matrix elements the final-state wave function includes the interaction of each one of the two outgoing nucleons with the residual nucleus by means of a phenomenological optical potential [27]. The nuclear current is the sum of a one-body and of a two-body part, including terms corresponding to the lowest order diagrams with one-pion exchange, namely seagull, pion-in-flight, and those with intermediate  $\Delta$  isobar configurations for  $np$  knockout. For  $pp$  knockout only the terms corresponding to diagrams with intermediate  $\Delta$  isobar configurations and without charge exchange contribute to the two-body current.

The two-nucleon overlaps between the ground state of  $^{16}\text{O}$  and the lowest-lying discrete final states of  $^{14}\text{C}$  and  $^{14}\text{N}$  are obtained from two different but similar approaches, based on the Brueckner  $G$ -matrix for  $pp$  pairs [26,2] and on the coupled cluster method for  $np$  pairs [3]. In both cases the overlaps are expressed in terms of a sum over relative and cm wave functions. The coefficients in the sum are obtained in the  $pp$  case from structure calculations in an extended shell-model space large enough to incorporate the corresponding collective features that influence the pair removal amplitude. The s.p. propagators used for this description of the two-particle propagators also include the effect of

both long-range correlations and SRC. In the  $np$  case the expansion coefficients are determined from a configuration mixing calculations of the two-hole states in  $^{16}\text{O}$ , which can be coupled to the angular momentum and parity of the requested state and are renormalized to account for the spectroscopic factors of the s.p. states. SRC, and also tensor correlations for  $np$  pairs, are included by the addition of state dependent defect functions to the uncorrelated radial partial waves of the relative motion. The defect functions were obtained for  $pp$  pairs by solving the Bethe-Goldstone equation and for  $np$  pairs within the framework of the coupled cluster method.

Different types of correlations are contained in the overlap functions, with some approximations but consistently. Therefore the spectroscopic factor is already included in the calculation. This allows a direct comparison with data, without the need to apply a reduction factor, accounting for the correlations not included in the model, as it is usually done in the analysis of  $(e, e'p)$  data.

The results of this model are in reasonable agreement with cross section data for the  $^{16}\text{O}(e, e'pp)^{14}\text{C}$  reaction [4–8]. The comparison has given clear evidence for SRC for the transition to ground state of  $^{14}\text{C}$ .

The experimental separation of the various structure functions in the  $(\vec{e}, e'\vec{p}\vec{p})$  reaction appears extremely difficult. A measurement of the components of  $\mathbf{P}$  and  $\mathbf{P}'$ , at least in particular situations, would be simpler and less affected by experimental errors, as it is obtained through the determination of asymmetries. One can expect that in the polarizations can be emphasized effects that are smoothed out in the cross section or that vice versa, owing to the ratio, can be smoothed out effects that are important in the cross section. Thus, a combined investigation of cross sections and polarizations would give complementary information.

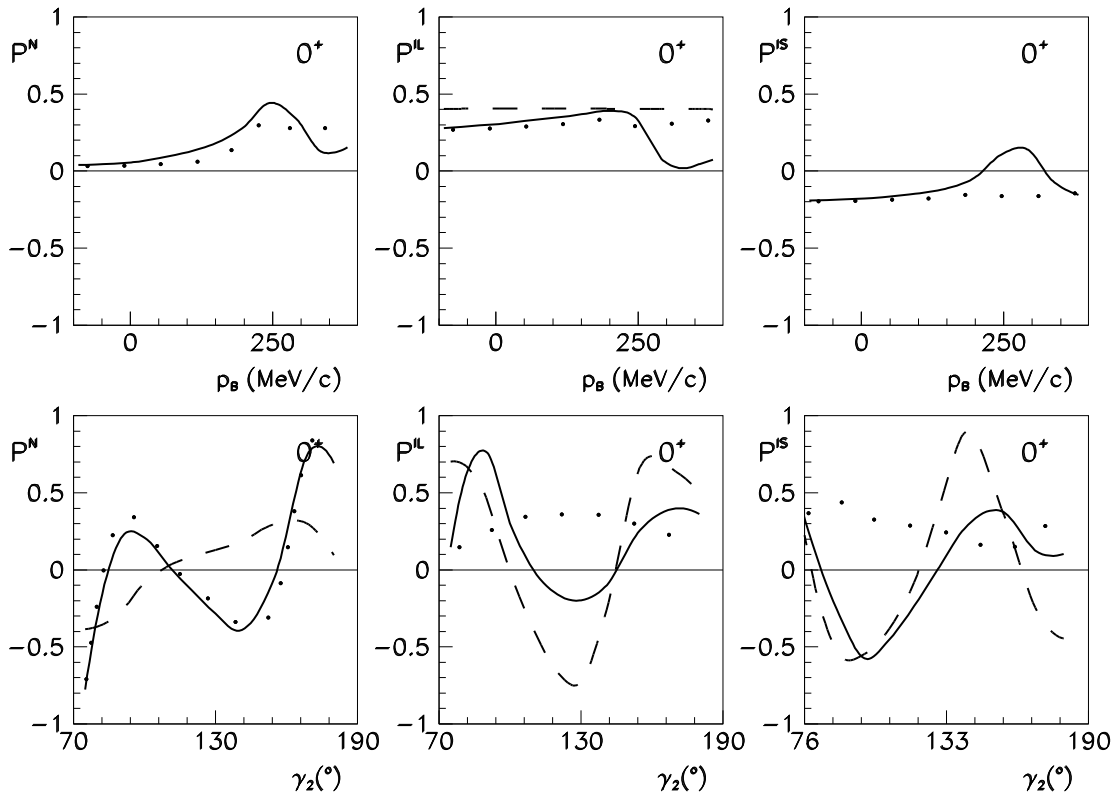


FIG. 1. The components  $P^N$ ,  $P^L$  and  $P^S$  of the  $^{16}\text{O}(\vec{e}, e'\vec{p}\vec{p})^{14}\text{C}$  reaction for the transition to the  $0^+$  ground state of  $^{14}\text{C}$ . Polarization is considered for the proton characterized by the momentum  $\mathbf{p}'_1$ . The dotted lines give the separate contribution of the one-body current, the dashed lines the one of the two-body  $\Delta$  current and the solid line the total result. The defect functions for the Bonn-A  $NN$  potential are used. In the upper panels a super-parallel kinematics ( $\gamma_1 = 0^\circ$ ,  $\gamma_2 = 180^\circ$ ) is calculated with  $E_0 = 855$  MeV,  $\omega = 215$  MeV and  $q = 316$  MeV/c. Different values of the recoil momentum  $p_B$  are obtained changing the kinetic energies of the outgoing protons. Positive (negative) values of  $p_B$  refer to situations where  $\mathbf{p}_B$  is parallel (antiparallel) to  $\mathbf{q}$ . In the lower panels a coplanar kinematics is considered, with  $E_0 = 584$  MeV,  $\omega = 212$  MeV and  $q = 300$  MeV/c,  $T'_1 = 137$  MeV and  $\gamma_1 = 30^\circ$ , on the opposite side of the outgoing electron with respect to the momentum transfer.

A numerical example for the components of  $\mathbf{P}$  and  $\mathbf{P}'$  in the  $^{16}\text{O}(\bar{e}, e'\bar{p}p)^{14}\text{C}_{\text{g.s.}}$  reaction is shown in Fig. 1. Results are compared for two coplanar kinematics considered in the cross section measurements at MAMI and NIKHEF. In coplanar kinematics only the components  $P^N$ ,  $P'^L$  and  $P'^S$  survive. The results for the super-parallel kinematics in the upper panels are of particular interest, because there are plans to measure polarization in this kinematics at MAMI [28]. In the super-parallel kinematics, where only one structure function contributes to each component,  $P^N$ ,  $P'^L$ , and  $P'^S$  are in general smaller than in the calculations displayed in the lower panels, where more structure functions contribute. All the polarization components are anyhow sizable in both kinematics.

For the considered transition and in both kinematics the cross sections are dominated by the one-body current and thus by SRC [2]. The contribution of the  $\Delta$  current becomes relevant only at large values of  $p_B$ , beyond 200 MeV/c. The dominant role of SRC is confirmed in Fig. 1 for  $P^N$  in both kinematics. Like for the cross section, the  $\Delta$  current is relevant only at large values of  $p_B$ . Thus, a measurement of  $P^N$  would give information on SRC. However, since  $\mathbf{P}$  is entirely due to FSI, it might be also sensitive to their theoretical treatment. The role of the  $\Delta$  current is more important on  $P'^L$  and  $P'^S$ , especially for the kinematics considered in the lower panels. A measurement appears more difficult in this case, since it requires also a polarized incident electron.

The results given by the two sets of defect functions from Bonn-A and Reid potentials are compared in Fig. 2. In the considered kinematics the two sets give cross sections with the same shape, while the magnitude is reduced by a factor of about 2 with Reid [2]. The results for the components  $P^N$ ,  $P'^L$ , and  $P'^S$  are qualitatively similar, but there are also appreciable differences. This is an indication that cross sections and polarization components can have a different sensitivity to the treatment of correlations.

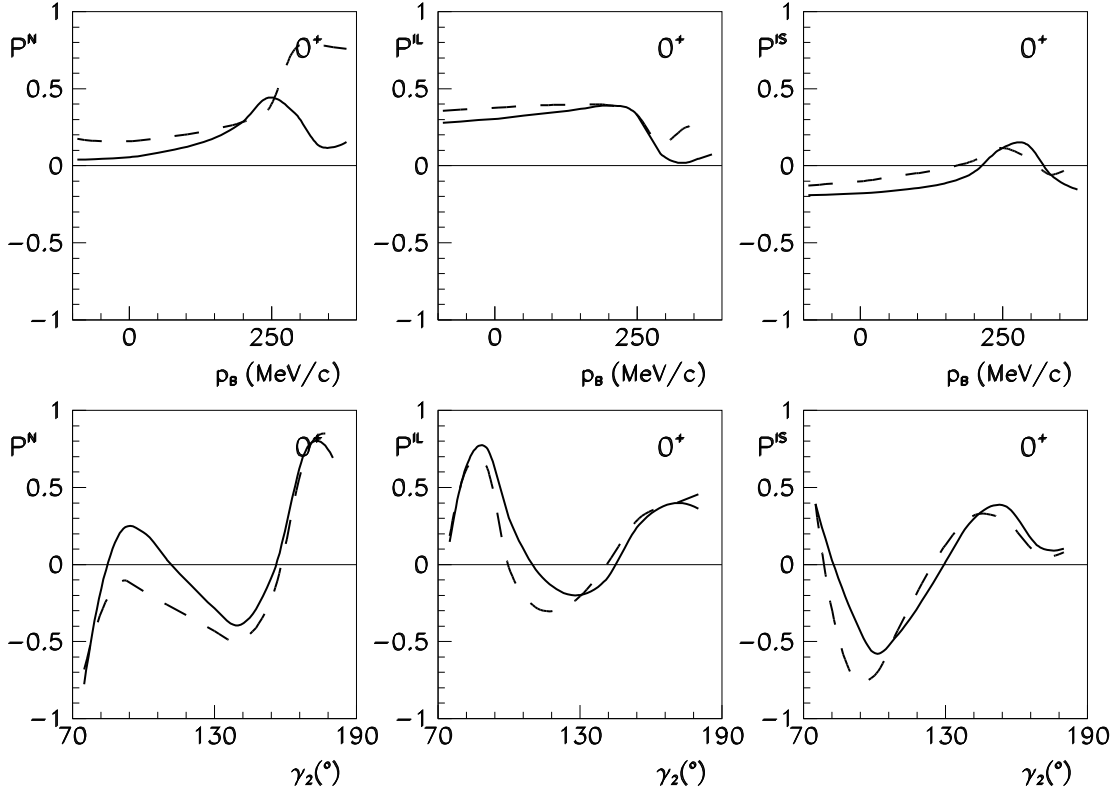


FIG. 2. The components  $P^N$ ,  $P'^L$  and  $P'^S$  for the same reaction and the same kinematics in upper and lower panels as in Fig. 1. The defect functions for the Bonn-A and Reid  $NN$  potentials are used in the solid and dashed lines, respectively.

In Fig. 3  $P^N$ ,  $P^L$ , and  $P^S$  are displayed for the  $^{16}\text{O}(\bar{e}, e'\bar{n}p)^{14}\text{N}_{g.s.}$  reaction in the same kinematics as in Fig. 1. The analysis of this reaction would be useful for testing the theoretical description of the two-body currents and obtaining information on the properties of tensor correlations. Both contributions are relevant in this case and the results are influenced by all the components of the nuclear current. Correlations are important in particular situations, for instance on  $P^N$  and  $P^S$  in the super-parallel kinematics, where anyhow these quantities are rather small.

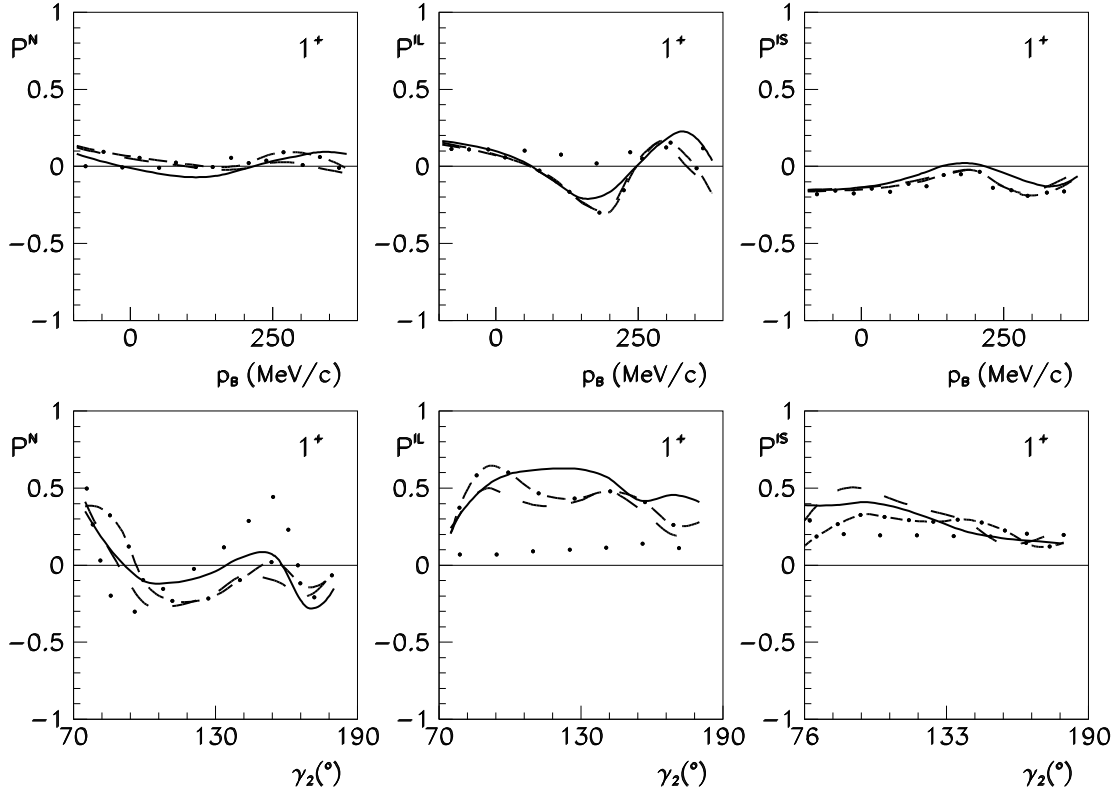


FIG. 3. The components  $P^N$ ,  $P^L$  and  $P^S$  of the  $^{16}\text{O}(\bar{e}, e'\bar{n}p)^{14}\text{N}$  reaction for the transition to the  $1^+$  ground state of  $^{14}\text{N}$ . Kinematics in upper and lower panels as in Fig. 1. Defect functions for the Argonne V14 potential are used. The separate contributions given by the one-body currents (dotted lines), the sum of the one-body and seagull currents (dot-dashed lines), the sum of the one-body, seagull and pion-in-flight currents (dashed lines) are displayed. The solid lines give the final results, where also the  $\Delta$  current is added.

The 16 structure functions obtained in the  $(\vec{\gamma}, \vec{N}N)$  reaction are directly connected with 16 measurable quantities. A complete study requires out-of-plane kinematics. Some examples can be found in [23]. Here a simpler coplanar kinematics is considered with an incident photon energy  $E_\gamma = 120$  MeV. The calculated unpolarized differential cross section and the 7 polarization observables are displayed in Figs. 4 and 5 for the  $^{16}\text{O}(\vec{\gamma}, \vec{p}\vec{p})^{14}\text{C}_{\text{g.s.}}$  reaction. The value of the photon energy, far from the peak of the  $\Delta$  resonance, has been chosen in order to reduce the contribution of the two-body  $\Delta$  current, that is an interesting but difficult ingredient of the theoretical model. Both SRC and two-body currents are important in general. Anyhow either process can prevail or can be even dominant for different polarization observables and in particular kinematics. In Fig. 4 SRC are of particular relevance on the unpolarized cross section at larger values of  $\gamma_2$ , while the  $\Delta$  gives the major contribution at lower values of  $\gamma_2$ . A similar result is obtained for  $P^N$ . The two-body  $\Delta$  current plays the main role on  $P_c^L$  and  $P_c^S$ , although the final result is different from the two separate contributions. In Fig. 5  $\Sigma_{\pi/2}^N$  and  $\Sigma_{\pi/4}^S$  are mainly driven by SRC, while the  $\Delta$  current prevails in  $\Sigma_{\pi/4}^L$ . The role of SRC is very important also on the photon asymmetry  $\Sigma_{\pi/2}$ . Some of these observables,  $P^N$ ,  $\Sigma_{\pi/2}^N$ ,  $\Sigma_{\pi/4}^L$ , and  $\Sigma_{\pi/4}^S$ , vanish in the PW approximation and might thus be useful to investigate FSI. This example indicates that a combined study of the cross section and polarization observables would provide an interesting tool to unravel and separately investigate the different contributions.

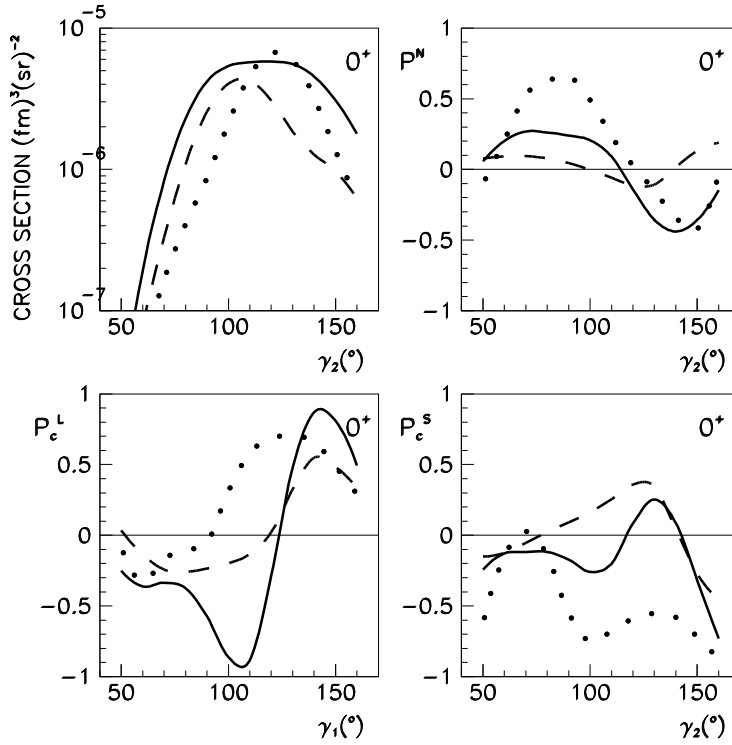


FIG. 4. The unpolarized differential cross section  $\sigma_0$  and the polarization observables  $P^N$ ,  $P_c^L$ , and  $P_c^S$  of the  $^{16}\text{O}(\vec{\gamma}, \vec{p}\vec{p})^{14}\text{C}_{\text{g.s.}}$  reaction in a coplanar kinematics with  $E_\gamma = 120$  MeV,  $T_1' = 45$  MeV and  $\gamma_1 = 45^\circ$ . Defect functions and line convention as in Fig. 2.



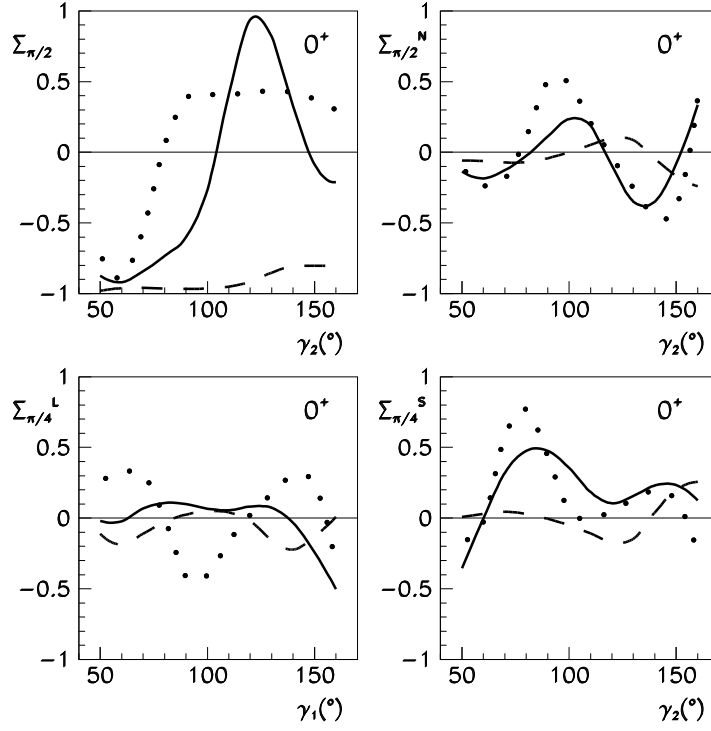


FIG. 5. The polarization observables  $\Sigma_{\pi/2}$ ,  $\Sigma_{\pi/2}^N$ ,  $\Sigma_{\pi/4}^L$ , and  $\Sigma_{\pi/4}^S$  for the same reaction, in the same conditions and kinematics and with the same line convention as in Fig. 4.

This result is confirmed also by the results obtained for the  $^{16}\text{O}(\vec{\gamma}, \vec{n}p)^{14}\text{N}$  reaction [23]. In this case the role of all the different terms of the two-body current is in general more relevant than in  $pp$  knockout, but the different sensitivity of the various polarization observables to the theoretical ingredients, i.e. to the nuclear current, FSI, and to the treatment of  $NN$  correlations and nuclear structure effects in the two-nucleon overlap function, is confirmed. Moreover, different effects can be emphasized in suitable kinematics.

In conclusion, the study of cross sections and polarizations in electron and photon-induced knockout reactions would result in a stringent test of the theoretical models and would provide an unique tool to shed light on the genuine nature of correlations in nuclei.

- [1] S. Boffi *et al.*, *Electromagnetic Response of Atomic Nuclei*, Oxford Studies in Nuclear Physics (Clarendon Press, Oxford, 1996).
- [2] C. Giusti *et al.*, *Phys. Rev. C* **57** (1998) 1691.
- [3] C. Giusti *et al.*, *Phys. Rev. C* **60** (1999) 054608.
- [4] C. J. G. Onderwater *et al.*, *Phys. Rev. Lett.* **78** (1997) 4893.
- [5] C. J. G. Onderwater *et al.*, *Phys. Rev. Lett.* **81** (1998) 2213.
- [6] R. Starink, *Phys. Lett. B* **474** (2000) 33.
- [7] G. Rosner, *Proc. of Conf. on "Perspectives in Hadron Physics"*, eds. S. Boffi *et al.*, World Scientific. Singapore (1998) p.185.
- [8] G. Rosner, *Prog. Part. Nucl. Phys.* **44** (2000) 99.
- [9] P. Grabmayr *et al.*, MAMI proposal A1-5/98, Mainz 1998.
- [10] J. Arends *et al.*, *Z. Phys. A* **298** (1980) 103.
- [11] M. Kanazawa *et al.*, *Phys. Rev. C* **35** (1987) 1828.
- [12] J. C. McGeorge *et al.*, *Phys. Rev. C* **51** (1995) 1967;  
P. Grabmayr *et al.*, *Phys. Lett. B* **370** (1996) 17;  
P. D. Harty *et al.*, *Phys. Lett. B* **380** (1996) 247;  
T. Lamparter *et al.*, *Z. Phys. A* **355** (1996) 1;  
I. J. D. MacGregor *et al.*, *Phys. Rev. Lett.* **80** (1998) 245;  
D. P. Watts *et al.*, *Phys. Rev. C* **62** (2000) 014616.
- [13] L. Isaksson *et al.*, *Phys. Rev. Lett.* **83** (1999) 3146.
- [14] P. Grabmayr *et al.*, MAMI proposal A2-4/97, Mainz 1997.
- [15] P. Grabmayr, *Proc. of the Fourth Workshop on Electromagnetically Induced Two-Nucleon Emission*, eds. A. Lallena and P. Grabmayr, Granada (1999) p. 331.
- [16] C. Giusti *et al.*, *Nucl. Phys. A* **546** (1992) 607; *Nucl. Phys. A* **564** (1993) 473.
- [17] C. Giusti and F. D. Pacati, *Nucl. Phys. A* **641** (1998) 297.
- [18] J. Ryckebusch *et al.*, *Phys. Rev. C* **57** (1998) 1318.
- [19] D. J. Tedeschi *et al.*, *Phys. Rev. Lett.* **73** (1994) 408.
- [20] H. Baghaei *Proc. of the Second Workshop on Electromagnetically Induced Two-Nucleon Emission*, eds. J. Ryckebusch and M. Waroquier, Gent (1995) p. 195.
- [21] I. J. D. MacGregor, *Proc. of the Fourth Workshop on Electromagnetically Induced Two-Nucleon Emission*, eds. A. Lallena and P. Grabmayr, Granada (1999) p. 339.
- [22] C. Giusti and F. D. Pacati, *Phys. Rev. C* **61**, (2000) 054617.
- [23] C. Giusti and F. D. Pacati, nucl-th/0102036.
- [24] J. Ryckebusch *et al.*, *Phys. Lett. B* **441** (1998) 1.
- [25] C. Giusti and F. D. Pacati, *Nucl. Phys. A* **535** (1991) 573; *Nucl. Phys. A* **571** (1994) 694.
- [26] W. J. W. Geurts *et al.*, *Phys. Rev. C* **54** (1996) 1144.
- [27] A. Nadasen *et al.*, *Phys. Rev. C* **23** (1981) 1023.
- [28] M. Distler, contribution to this workshop.